ErpA, an iron–sulfur (Fe–S) protein of the A-type essential for respiratory metabolism in *Escherichia coli*

Laurent Loiseau*, Catherine Gerez†, Martijn Bekker‡, Sandrine Ollagnier-de Choudens†, Béatrice Py*, Yannis Sanakis§, Joost Teixeira de Mattos‡, Marc Fontecave†, and Frédéric Barras*¶

*Unité Propre de Recherche 9043, Laboratoire de Chimie Bactérienne, Centre National de la Recherche Scientifique, 31 Chemin Joseph Aiguier, 13402 Marseille Cedex 20, France; †Unité Mixte de Recherche 5249, Institut de Recherches en Technologies et Sciences pour le Vivant/Laboratoire de Chimie et Biologie des Métaux, Centre Energie Atomique/Centre National de la Recherche Scientifique/Université Joseph Fourier, 17 Avenue des Martyrs, 38054 Grenoble Cedex 09, France; ‡Department of Molecular and Microbial Physiology, Swammerdam Institute of Life Sciences, University of Amsterdam, 166 Nieuwe Achtergracht, 1018WV, Amsterdam, The Netherlands; and §Institute of Materials Science, National Center for Scientific Research ''Demokritos,'' 153 10 Agia Paraskevi, Attiki, Greece

Communicated by Helmut Beinert, University of Wisconsin, Madison, WI, June 22, 2007 (received for review January 30, 2007)

Understanding the biogenesis of iron–sulfur (Fe–S) proteins is relevant to many fields, including bioenergetics, gene regulation, and cancer research. Several multiprotein complexes assisting Fe–S assembly have been identified in both prokaryotes and eukaryotes. Here, we identify in *Escherichia coli* an A-type Fe–S protein that we named ErpA. Remarkably, *erpA* was found essential for growth of *E. coli* in the presence of oxygen or alternative electron acceptors. It was concluded that isoprenoid biosynthesis was impaired by the *erpA* mutation. First, the eukaryotic mevalonate-dependent pathway for biosynthesis of isopentenyl diphosphate restored the respiratory defects of an *erpA* mutant. Second, the *erpA* mutant contained a greatly reduced amount of ubiquinone and menaquinone. Third, ErpA bound Fe–S clusters and transferred them to apo-IspG, a protein catalyzing isopentenyl diphosphate biosynthesis in *E. coli*. Surprisingly, the *erpA* gene maps at a distance from any other Fe–S biogenesis-related gene. ErpA is an A-type Fe–S protein that is characterized by an essential role in cellular metabolism.

essential gene *yadR* | isoprenoid | respiration | scaffold

Iron–sulfur (Fe–S) proteins are crucial for prokaryotic and eukaryotic cell metabolism (1–5). They carry out tasks related to numerous biological processes, ranging from electron transfer to DNA repair. The successful use of Fe–S clusters as cofactors in a large series of unrelated proteins is best explained by both chemical and evolutionary considerations. Chemical considerations point to the fact that Fe–S clusters can accept or donate electrons and thus have become involved as cofactors in electron transfer systems. Furthermore, they are strong Lewis acids and are therefore suitable for substrate activation in nonredox enzymes. Evolutionary considerations rest on the fact that Fe and S were present in abundance during the early stages of life, facilitating their recruitment as cofactors by ancient enzymes.

In both prokaryotes and eukaryotes, severe phenotypic defects have been found to be caused by the inability of the cells to build Fe–S proteins. For instance, clinically relevant mutations in patients with trichothiodystrophy and Fanconi anemia disrupt the Fe–S clusters of XPD (xeroderma pigmentosum group D) and FancJ helicases (6). In addition, it has been pointed out that there is a connection between dysfunctioning of Fe–S biogenesis machineries and neurodegenerative diseases (1). Furthermore, in bacterial pathogens, defects in Fe–S biogenesis led to a reduction in virulence (7, 8). Not surprisingly, in the last decade, interest regarding how apoproteins acquire their Fe–S cluster *in vivo* has arisen in several disciplines in biology.

Studies in both prokaryotes and eukaryotes led to the discovery of several multiprotein complexes, referred to as ISC, SUF, and NIF, that are necessary for building and inserting Fe–S clusters into cellular targets (1–5). A pioneering investigation of the *Azotobacter vinelandii* NIF system led to the emergence of the cysteine desulfurase/scaffold duo as the minimal toolbox for making Fe–S clusters *in vivo* (4, 9, 10). Cysteine desulfurases provide sulfur from L-cysteine (11). Scaffolds are defined as being able to bind both iron and sulfur so that a Fe–S cluster can form before being transferred to targeted apoproteins (12–18). The SUF system includes an atypical cytosolic ABC-type transporter that functions with the cysteine desulfurase for increasing the production of sulfur (19, 20). The ISC system includes chaperones that might activate Fe–S cluster transfer from the scaffold proteins to the targets and a ferredoxin of unknown function (21–25).

E. coli contains both the ISC and SUF systems (2–4). Each system contains a so-called A-type scaffold protein. It has been shown that A-type proteins bind either $[2Fe–2S]^{2+}$ or $[4Fe–4S]^{2+}$ clusters and transfer them to apoproteins (14–18). Three conserved Cys residues could act as ligands for these clusters, as indicated by mutagenesis studies and by the recently obtained 3D structure of IscA (26–29). However, the proposal that IscA/SufA acts as a scaffold was challenged by *in vitro* studies, which suggest that A-type proteins act as iron chaperones, and by the fact that mutations in *iscA* or *sufA* did not yield major physiological defects (30–36). Noticeably, however, in *A. vinelandii*, *iscA* appeared to be required at high concentrations of oxygen (37).

In this study, we discovered an A-type Fe–S protein. The structural gene, which we named *erpA* (for essential respiratory protein A), is distant from any of the Fe–S biogenesis operons. Remarkably, *erpA* was found to be essential for *E. coli* to grow in the presence of oxygen or other electron acceptors. Biochemical, metabolic, and genetic analyses allowed us to identify the isopentenyl diphosphate (IPP) biosynthesis pathway requiring ErpA function.

Results

Identification of ErpA, a Putative A-Type Fe–S Protein in *E. coli*. BLAST analysis of the *E. coli* genome using *iscA* and/or *sufA* as queries uncovered *yadR*, a gene of unknown function. The predicted YadR primary sequence exhibits 40% identity with IscA and 34% identity with SufA, including the three strictly conserved Cys residues that are essential for A-type function

Author contributions: L.L., C.G., M.B., S.O.-d.C., Y.S., and F.B. designed research; L.L., C.G., M.B., and Y.S. performed research; L.L., C.G., M.B., S.O.-d.C., B.P., J.T.d.M., M.F., and F.B. analyzed data; and L.L., C.G., M.B., S.O.-d.C., B.P., J.T.d.M., M.F., and F.B. wrote the paper.

The authors declare no conflict of interest.

Abbreviations: IPP, isopentenyl diphosphate; MVA, mevalonate.

¶To whom correspondence should be addressed: E-mail: barras@ibsm.cnrs-mrs.fr.

This article contains supporting information online at www.pnas.org/cgi/content/full/0705829104/DC1.

[supporting information (SI) Fig. 6]. This sequence-based information suggested that YadR was a new Fe–S protein of the A type. Subsequent experiments confirmed this, and from now on, we propose to name this gene *erpA* (essential respiratory protein A).

ErpA Binds Both [2Fe–2S] and [4Fe–4S] Clusters. Large quantities of a soluble His-tagged ErpA protein were purified from *E. coli*. ErpA eluted from a gel filtration column in a major peak corresponding to a dimer (data not shown). Purified solutions of ErpA were slightly pink-colored, with a UV-visible spectrum displaying absorption bands in the 300- to 450-nm region. Iron and sulfide were present in stoichiometric amounts, but with <0.1 iron and sulfide per polypeptide chain. ApoErpA incubated with a 4-fold molar excess of both ferrous iron and sulfide under anaerobic and reducing conditions yielded a brownish protein that contained a maximum amount of 1.5–2 atoms of iron and sulfide per polypeptide chain, i.e., holoErpA. The UV-visible spectrum of holoErpA displayed absorption bands at 325, 420, and 460 nm, indicating the presence of Fe–S clusters (data not shown).

Mössbauer spectroscopy was used to characterize the nature of the iron sites present in holoErpA. The reconstituted protein was prepared with $^{57}FeCl_3$/DTT, and the sulfide was provided by the IscS-dependent cysteine desulfurization reaction. The Mössbauer spectra recorded at 4.2 K and 110 K are shown in SI Fig. 7. Three different quadrupole doublets are identified at 4.2 K. The first major doublet (trace 1 in SI Fig. 7) has parameters consistent with a $[2Fe–2S]^{2+}$ cluster, i.e., isomer shift, $\delta = 0.28$ mm/s and quadruple splitting, $\Delta E_Q = 0.58$ mm/s. This assignment is further supported by the fact that the behavior of this doublet is consistent with an $S = 0$ ground state. The behavior of the second site (trace 2 in SI Fig. 7) also is consistent with a diamagnetic ground state and, based on its parameters ($\delta = 0.48$ mm/s and $\Delta E_Q = 1.11$ mm/s), is attributed to a $[4Fe–4S]^{2+}$ cluster. The third doublet (trace 3 in SI Fig. 7) has parameters ($\delta = 0.70$ mms and $\Delta E_Q = 3.28$ mm/s) typical for Fe^{2+} ($S = 2$) mononuclear species in a tetrahedral environment comprising sulfur atoms. This site is attributed to contamination. These three doublets are superimposed on a broad background spectrum extending from −6 mm/s to +2.2 mm/s, which is attributed to paramagnetic ferric impurities. In the spectrum at 110 K (SI Fig. 7) the broad signal collapses into a quadrupole doublet (trace 4 in SI Fig. 7), which overlaps significantly with the doublet from the $[4Fe–4S]^{2+}$ cluster. Approximate parameters for doublet 4 are $\delta = 0.60$ mm/s and $\Delta E_Q = 1.04$ mm/s. From an analysis of the spectra at both temperatures, we estimate that ≈10% of the iron corresponds to high-spin mononuclear ferrous iron, 40–50% belongs to $[2Fe–2S]^{2+}$ clusters, 15–25% corresponds to $[4Fe–4S]^{2+}$ clusters, and the remaining iron corresponds to the paramagnetic species. Similar results were obtained with a sample of ErpA protein with no His tag; the only difference was the reduced amount of high-spin ferrous iron (data not shown). These results demonstrate that ErpA can assemble both [2Fe–2S] and [4Fe–4S] clusters, as observed for IscA and SufA proteins (14–16).

The *erpA* Gene Is Essential for Growth Under Aerobic Conditions. To investigate its physiological role, we sought to inactivate the *erpA* gene. However, insertion of a cassette into the *erpA* gene proved to be impossible unless the cells had duplicated a wild-type allele, a situation typically encountered when trying to inactivate essential genes (data not shown). Therefore, we constructed a conditional mutant in which the expression of the *erpA* gene was under arabinose induction and glucose repression. The resulting strain, referred to as LL401 (*ara*$_p$::*erpA*), grew normally only when arabinose was in the medium (Fig. 1*A*). LL401 was transformed with either pUC18 or pLUE-A, a pUC18-derived plasmid carrying the *erpA* gene. Cultures were grown overnight in the presence of arabinose, washed, and used to inoculate fresh medium containing either arabinose or glucose. In the presence of glucose, the LL401/pUC18 strain ceased growing, whereas LL401/pLUE-A grew normally (Fig. 1*B*).

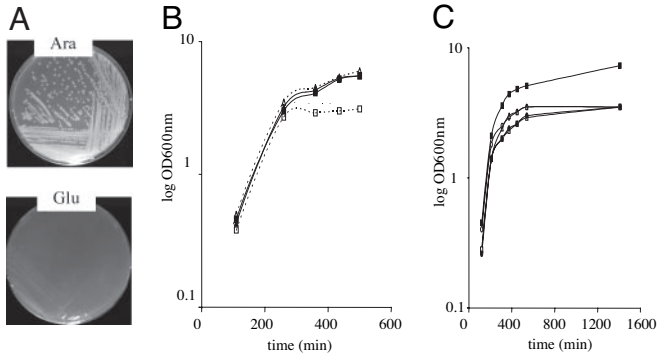

Fig. 1. Growth analysis of *E. coli* LL401(*ara*$_p$::*erpA*) strain in aerobiosis. (*A*) Strain LL401 was grown on LB medium plates with added arabinose (Ara) (*Upper*) or glucose (Glu) (*Lower*). (*B*) Strains were grown in LB medium with added 0.2% glucose (broken lines and open symbols) or 0.2% arabinose (solid lines and filled symbols). The strains studied were LL401(*ara*$_p$::*erpA*)/pUC18 (squares) and LL401(*ara*$_p$::*erpA*)/pLUE-A(*erpA*$^+$) (triangles). (*C*) Strains LL401(*ara*$_p$::*erpA*) harboring pUC18 (○), pLUE-A (■), pLUE-A42 (△), pLUE-A106 (□), and pLUE-A108 (●) were grown in LB medium with 0.2% glucose added.

Mutated versions of the *erpA* gene, in which codons corresponding to the three conserved cysteine residues were individually changed to serine codons, were constructed. All three plasmids carrying the cognate mutated genes *erpA-C42S*, *erpA-C106S*, and *erpA-C108S* failed to complement growth defects of the LL401 *erpA* mutant (Fig. 1*C*). Together, these results indicate that *erpA* was essential for *E. coli* to grow under aerobic conditions and that the conserved cysteine residues are important for the function of the protein *in vivo*.

The *erpA* Gene Is Essential for Anaerobic Respiration. Surprisingly, under fermentative conditions, the LL401 strain (*ara*$_p$::*erpA*) was found to grow in the presence of glucose, i.e., the growth condition repressing *erpA* expression (Fig. 2*A*). Therefore, we could exploit anaerobic conditions to construct a mutant lacking the whole *erpA* gene, referred to as LL402 (Δ*erpA*::*cat*). Although the LL402 strain was able to grow anaerobically in the presence of glucose, it was unable to grow in the presence of glycerol and either nitrate, trimethylamine *N*-oxide, or fumarate (Fig. 2*B*). These results indicate that a functional *erpA* gene is dispensable for fermentation but is essential for anaerobic respiration.

The Eukaryotic Mevalonate (MVA)-Dependent Pathway Allowed Growth of the *erpA* Mutant. We made the assumption that the respiration defect was related to alteration of quinone pools. Indeed, quinone derivatives are electron carriers used by both anaerobic and aerobic respiratory chains and are derived from IPP, whose synthesis in bacteria depends on two essential [4Fe–4S] cluster-containing proteins, namely IspG (formally GcpE) and IspH (formally LytB) (38, 39). The *erpA* null mutation (Δ*erpA*::*cat*) was introduced into an engineered *E. coli* strain, which can synthesize IPP both by its natural endogenous pathway and by the eukaryotic MVA-dependent pathway, a pathway that does not employ Fe–S enzymes (40). The resulting LL405 strain (Δ*erpA*::*cat*, MVA$^+$) grew on LB plates containing both MVA and arabinose, the substrate and the inducer, respectively, of the MVA-dependent pathway (Fig. 3*A*). In contrast, the LL402 strain failed to grow under these conditions (Fig. 3*A*). The same observation was obtained with strains growing in liquid cultures (Fig. 3*B*). Both the presence of MVA (Fig. 3*B*) and arabinose (data not shown) were necessary to allow growth of the LL405 strain. Together these experiments showed that IPP synthesis restored the inability of the

BIOCHEMISTRY

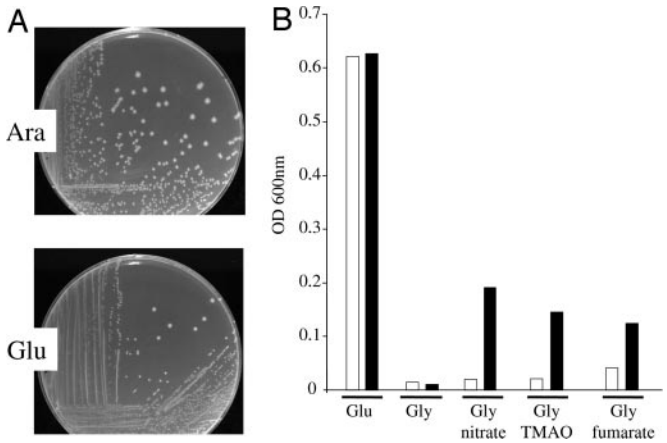

Fig. 2. Growth analysis of *E. coli* LL401(*ara*$_P$::*erpA*) and LL402 (Δ*erpA*::*cat*) strains in anaerobiosis. (*A*) Strain LL401 was grown on LB medium plates with added arabinose (Ara) (*Upper*) or glucose (Glu) (*Lower*). (*B*) Strains LL402(Δ*erpA*::*cat*)/pUC18 (open bars) and LL402(Δ*erpA*::*cat*)/pLUE-A (*erpA*$^+$) (filled bars) were grown under anaerobiosis in minimal medium supplemented with glucose or glycerol as a carbon source and with nitrate, trimethylamine *N*-oxide (TMAO), or fumarate as electron acceptors. The inoculum was 0.02 ml of an overnight culture grown under anaerobiosis in minimal medium with glucose. Cells were pelleted and washed before inoculation. OD_{600} values were recorded after 16 h of incubation at 37°C. The experiment was performed in triplicate, and a representative experiment is shown.

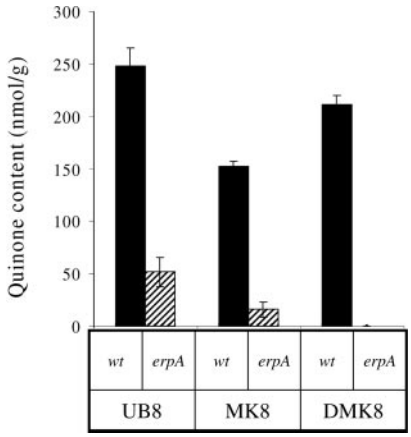

Fig. 4. Quinone contents from *E. coli* LL402 (Δ*erpA*::*cat*) and wild-type (wt) strains. Strains MG1655 and LL402 (Δ*erpA*::*cat*) were grown for 15 h under anaerobiosis in LB glucose medium. Two milliliters of the culture was taken, and cells were pelleted after three washes with water, resuspended in 4 ml of LB glucose, and incubated 2 h at 37°C under aerobiosis, then cells were washed three times, pelleted, and frozen directly. Ubiquinone (UB8), menaquinone (MK8), and dimethylmenaquinone (DMK8) contents in the samples from MG1655 (black bars) and LL402 (Δ*erpA*::*cat*) (hatched bars) were determined.

mutant to grow under respiratory conditions and suggested that ErpA participates in IspG/IspH maturation.

The *erpA* Mutant Contains a Reduced Amount of Quinone. Depletion of IPP is expected to affect quinone synthesis. Therefore we investigated whether *erpA* mutation led to a modification of the quinone pool. Wild-type and LL402 (Δ*erpA*::*cat*) strains were grown overnight under fermentative conditions and shifted to aerobiosis. Samples were taken 2 h after the shift, and the amount of quinone was quantitated (Fig. 4). Ubiquinone (UQ8) synthesis was reduced 5-fold in the mutant compared with the wild type. In addition, the mutant contained 6-fold less menaquinone than the wild type and contained no dimethylmenaquinone at all. Taken together, these results show that *erpA* mutation causes a drastic alteration of quinone synthesis.

ErpA Is Able to Transfer Clusters to IspG *in Vitro*. We next tested whether ErpA could insert Fe–S clusters into apo-IspG. The IspG protein was purified and isolated in its apo-form (apoIspG). The apoIspG protein was incubated anaerobically with a 2.2-fold excess of ^{57}Fe-reconstituted ErpA. After 1 h of reaction, IspG was separated from ErpA onto a Superdex 200 gel filtration column and further analyzed by UV-visible and Mössbauer spectroscopies, as well as for its Fe content. This preparation, presumably holoIspG containing approximately four Fe atoms per polypeptide chain, had an absorption band at 410 nm, characteristic of a [4Fe–4S] cluster (Fig. 5*A*). The Mössbauer spectrum recorded at 4.2 K (Fig. 5*B*) showed a slightly asymmetric doublet (97% relative area), which is consistent with a $[4Fe–4S]^{2+}$ ($S = 0$) cluster. This species was simulated with two doublets, I and II, at a 3:1 ratio as indicated by Seeman *et al.* (41). The analysis gave the following parameters for these doublets: I, $\delta = 0.47$ mm/s and $\Delta E_Q = 1.00$ mm/s and for doublet II, $\delta = 0.48$ mm/s and $\Delta E_Q = 1.34$ mm/s. The rest of the iron (3%) gave rise to doublet III, with parameters $\delta = 1.11$ mm/s and $\Delta E_Q = 2.70$ mm/s, which corresponds to a ferrous impurity. These results showed that IspG can be correctly matured by building a [4Fe–4S] cluster during reaction with holoErpA, in agreement with the hypothesis that ErpA is a Fe–S protein of the A type.

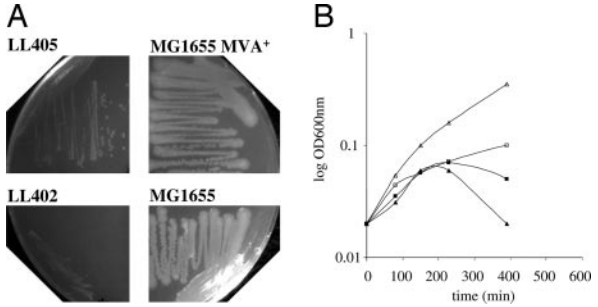

Fig. 3. Phenotypic suppression of *E. coli* LL402 (Δ*erpA*::*cat*) mutant by the eukaryotic MVA pathway. (*A*) Strains MG1655, MG1655 MVA$^+$, LL402 (Δ*erpA*::*cat*), and LL405 (Δ*erpA*::*cat*, MVA$^+$) were grown on an LB medium plate containing the MVA pathway inducer L-arabinose (0.2%) and the MVA substrate (1 mM) and was incubated at 37°C for 24 h under aerobiosis. (*B*) Strains LL402 (Δ*erpA*::*cat*) (square) and LL405 (Δ*erpA*::*cat*, MVA$^+$) (triangle) were grown under aerobiosis in 0.2% LB arabinose-containing medium supplemented (open symbols) or not (filled symbols) with 1 mM MVA.

Discussion

Traditionally, the studies of Fe–S proteins have been a central theme of bioenergetics, although in recent years new and unexpected connections between Fe–S proteins and topics, such as cancer research or bacterial pathogenicity, have emerged (1–5). As a consequence, the mechanism proteins use to acquire their Fe–S clusters has become an area of intense investigation. Likewise, an unsuspected complexity has been uncovered, and numerous proteins, conserved in prokaryotes and eukaryotes, that are required for building, inserting, or protecting Fe–S clusters have been identified. Here, we discovered ErpA, a protein that belongs to the class of so-called Fe–S A-type proteins, which assist Fe–S protein biogenesis in both prokaryotes and eukaryotes. In sharp contrast with other A-type Fe–S proteins, ErpA was found to perform an essential metabolic function. In particular, we were able to pinpoint its role in the biosynthesis of IPP, which is essential for the biochemistry of any living cell.

ErpA exhibits molecular properties closely related to those of the well characterized SufA and IscA proteins that have been

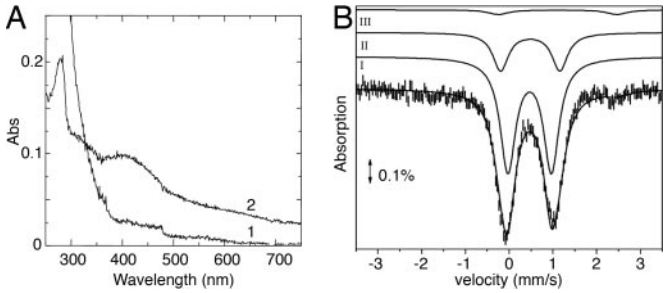

Fig. 5. Fe–S transfer from holoErpA to apo-IspG. (*A*) UV–visible light absorption spectra. ApoIspG (880 μM) (spectrum 1) was incubated anaerobically with 1.26 mM ^{57}Fe-reconstituted ErpA (two iron atoms per polypeptide chain) in 0.1 M Tris·HCl, pH 8/0.1 M NaCl/5 mM DTT for 1 h. Spectrum 2 shows reconstituted IspG after separation of proteins. (*B*) Mössbauer spectrum of 220 μM reconstituted IspG at 4.2 K. Solid lines above the spectra are theoretical simulations corresponding to the different doublets (see text).

proposed to act as scaffolds during Fe–S biogenesis: (*i*) Mössbauer spectroscopy analysis revealed that ErpA contained both $[2Fe–2S]^{2+}$ and $[4Fe–4S]^{2+}$ clusters; (*ii*) ErpA was able to transfer its cluster to apoIspG, a [4Fe–4S] protein; (*iii*) ErpA contained the A-type motif $CX_{63}CXC$; and (*iv*) the conserved Cys residues of A-type motif were required for ErpA to fulfill its function *in vivo*. Yet, in striking contrast with *sufA* and *iscA*, the absence of which yields no major phenotype, a functional *erpA* was found essential for *E. coli* to grow under conditions that allow either aerobic or anaerobic respiration.

Currently, the role of A-type proteins in Fe–S biogenesis is under debate. These proteins were initially proposed to be scaffolds, implying that they are able to bind both iron and sulfur to build a Fe–S cluster and eventually to transfer it to apoproteins. A challenge to the view of A-type proteins as scaffolds was recently raised by the finding that a double *iscA sufA* mutant of *Synechococcus* was viable, an observation *a priori* inconsistent with a pivotal role of A-type proteins in the maturation of cellular Fe–S proteins (36). Rather, in this study, IscA and SufA were proposed to receive preformed Fe–S clusters from Nfu protein and, eventually, to transfer these Fe–S clusters to SufR and IscR, two regulators. Nfu would thus be the actual scaffold, and, accordingly, Nfu was found to be essential in *Synechococcus* (36). In our case, such a model would imply that IscU, a demonstrated scaffold, would transfer a Fe–S cluster to ErpA, which in turn would assist IspG/H maturation. However, this scenario is not consistent with the observation that inactivating *iscU* does not confer a lethal phenotype under respiratory conditions. Models derived from studying one bacterial species are not always translatable to the understanding of other bacteria. For instance, an *iscA* mutation prevents *Azotobacter* growth under high oxygen tensions, whereas IscA is dispensable in *E. coli* under all studied conditions (37). Hence, we might expect a great diversity in the way bacteria make use of otherwise conserved components to carry out Fe–S biogenesis. Another challenge to the view of A-type proteins as scaffolds comes from *in vitro* investigations, which concluded that A-type proteins could be simple iron donors (30–34). Interestingly, the *erpA* gene is part of a chromosomal region that is particularly rich in iron uptake-related genes. The *fhuACDB* genes, which are involved in hydroxamate-dependent iron transport, and the *hemL* gene, which is involved in heme biosynthesis, are located upstream of the *erpA* gene, whereas downstream lies the *btuF* gene, which is involved in cobalamin uptake. Although this observation might be pure coincidence, it might be worth further investigation in the context of the view that A-type proteins serve as iron chaperones.

Several observations led us to propose that ErpA is implicated in IPP biosynthesis. First, an *erpA* mutant, which could not grow in the presence of oxygen, was rescued by introducing eukaryotic genes, which direct IPP synthesis from exogenously added MVA. Second, the *erpA* mutant was found to contain a reduced amount of quinones, whose synthesis is derived from IPP. IPP synthesis depends on two Fe–S proteins, namely IspG and IspH. Thus, the simplest hypothesis is that ErpA participates in Fe–S center acquisition of IspG and/or IspH. Accordingly, we showed that *in vitro* apoIspG could be matured by holoErpA. We noticed that the *erpA* strain synthesizing IPP by the eukaryotic MVA-dependent pathway grew much more slowly than the wild type, which may have been because the eukaryotic pathway was not functioning efficiently in *E. coli*, but this possibility was ruled out by showing that the MVA-dependent pathway allowed a strain devoid of either the *ispG* or the *ispH* gene to grow like the wild type (data not shown). Altogether, these observations indicate that ErpA participates in IPP biosynthesis but that a deficiency in IPP synthesis is not the sole phenotypic trait of the *erpA* mutant. By extension, we conclude that ErpA participates in the maturation of IspG and/or IspH and of as-yet-undetermined additional Fe–S proteins.

A clear defect of the *erpA* mutant was its inability to respire with either oxygen or alternative electron acceptors, such as nitrate, trimethylamine *N*-oxide, or fumarate, as terminal electron donors. A defect in aerobic respiration also was indicated by the failure of the *erpA* mutant to grow on glycerol and succinate (data not shown). Conversely, when grown fermentatively, the wild-type and the *erpA* mutant showed comparable quinone contents and growth rates (data not shown). This respiratory deficiency is consistent with a defect in IPP synthesis because IPPs are precursors of the quinones, key elements in the respiratory chain. However, the amount of ubiquinone found, although reduced several fold as compared with wild type, should still allow the *erpA* mutant to respire aerobically. Indeed, if one considers that the ubiquinone concentration in membranes of the *erpA* mutant is 600 μM (calculated from 50 nmol per gram of dry weight) (see Fig. 4) and the K_m for the major terminal oxidase (cytochrome bo type) for ubiquinol is 38 μM (42), whereas the K_m for the NADH dehydrogenase is $\approx$2 μM (43, 44), it must be concluded that the lowered ubiquinone concentration should not lead to complete inhibition of aerobic respiration in the *erpA* mutant. This raises the question of why the *erpA* mutant could not use respiration for growth in the presence of oxygen. A possibility is that additional Fe–S enzymes participating in the respiratory chain were inefficiently matured in the *erpA* mutant, which is consistent with the fact that the MVA-dependent pathway did not restore wild-type growth, as discussed in the paragraph above. The respiration defect would then reflect a sum of defects in different parts of the electron pathway.

IPPs play a general role in *E. coli* physiology. Indeed, besides quinones, IPPs are precursors for the synthesis of cell walls, hemes, and tRNA modifications. As a matter of fact, we observed filamentation of the *erpA* mutant under aerobic conditions but not under fermentation. This filamentation phenotype might well be caused by defects in cell wall biosynthesis. However, because the *erpA* mutant stops growing under aerobic conditions, it is hard to know whether filamentation is a consequence of the growth arrest or an additional consequence of the IPP biosynthesis defect. In any case, it is clear that the *erpA* mutant does not exhibit the pleitropic phenotype of an *ispG* or *ispH* mutant, which were unable to grow under any conditions tested.

E. coli makes use of ISC and SUF machineries for biogenesis and insertion of Fe–S clusters into apotargets. The role of the CSD system in Fe–S biogenesis needs to be ascertained (45). The *erpA* structural gene lies away from the SUF, ISC, or CSD systems encoding operons, but transcriptomic analysis identified *erpA* as a member of the IscR regulon (46). Expression of *erpA* is therefore coupled to that of the *sufABCDSE* and *iscRSUAhscBAfdx* operons. The question arises as to which machinery the ErpA protein interacts with. It would be interesting to study whether ErpA is a pleitropic component able to associate with the ISC, the SUF, or the

BIOCHEMISTRY

CSD systems or whether it is part of an as-yet-unidentified Fe–S biogenesis system.

In conclusion, this study has shown the case of an A-type Fe–S protein that plays an essential role in cellular viability in *E. coli*. Our work shows an occurrence of a lethal phenotype associated with a mutation in a single Fe–S biogenesis-related gene in *E. coli*. This functional importance is interpreted as reflecting a specific partnership between essential Fe–S enzymes to be matured, i.e., IspG and/or IspH at least, and ErpA, a dedicated A-type Fe–S protein. This leads us to predict that *in vivo*, cellular Fe–S proteins will be matured by a different set of ancillary proteins. Such a substrate specificity was not revealed by *in vitro* analyses. The next challenge would be to delineate such maturation-specific pathways as they occur *in vivo*.

Methods

Culture Media, Growth Conditions, and Chemicals. All chemicals were obtained from Sigma–Aldrich (St. Louis, MO) or Fluka (Buchs, Switzerland) unless otherwise stated. *E. coli* strains were grown in LB-rich medium or M9-based minimal medium at 37°C. Growth under anaerobiosis was achieved by using the GasPak Plus anaerobic system in a dedicated chamber. Ampicillin (50 μg/ml), kanamycin (25 μg/ml), spectinomycin (50 μg/ml), and chloramphenicol (25 μg/ml) were added when necessary. Arabinose or glucose were used at 0.2%, and glycerol was used at 0.4%. Fumarate (20 mM), nitrate (2 mM), and trimethyl amine oxide (20 mM) were used as electron acceptors. The strains are listed in SI Table 1.

Plasmids Construction. For expression of recombinant ErpA, the coding region of *erpA* was amplified from genomic DNA from the *E. coli* MG1655 strain by PCR with *Taq*DNA polymerase and primers NdeI-Us and XhoI-Uas (SI Table 2). The *erpA* product was digested and ligated in NdeI/XhoI linearized pET22b$^+$ to yield pET/ErpA, which was used for the expression of ErpA-His$_6$.

For a complementation test and/or mutant strain construction, the *erpA* gene was amplified by PCR from *E. coli* MG1655 chromosomal DNA using primers Es/Eas and inserted into pGEMT and pUC18 vectors (SI Table 1). pLUE-A106 and pLUE-A108 plasmids, containing either a Cys-to-Ser-106 mutation or a Cys-to-Ser-108 mutation, were constructed as follows. PCR products were obtained by using MG1655 chromosomal DNA with primers Es/Eas106S or Es/Eas108S. These products were digested with EcoRI/XhoI and inserted into pUC18 restricted by EcoRI/SalI. The pLUE-A42 plasmid was constructed as follows: PCR product was obtained by using pLUE-A DNA with primers EsC42S/inv lacZ 106S or Es/Eas108S. The PCR product was digested with AgeI/HindIII and inserted into pLUE-A digested with AgeI/HindIII. The pET/IspG plasmid was constructed by PCR amplification of MG1655 chromosomal DNA using primers NdeI ispG/XhoI Δstop ispG. The resulting PCR product was digested by NdeI/XhoI and inserted in pET22 plasmid. All constructs were checked by DNA sequence analysis.

Construction of the *erpA* Mutant Strains. The LL401 strain was constructed as follows. An insert carrying the *yadQ-aadA7*(Spc^R)-*araC-erpA* genes was obtained after three PCRs using overlapping oligonucleotides. Fragments *yadQ-aadA7*, *aadA7-araC*, and *araC-erpA* were obtained by using Q1/Q2, Sp1/Sp2, and pE1/Eas oligonucleotide pairs, mixed, and used as templates for a new PCR using the Q1/Eas oligonucleotide pair. This protocol made use of the TG1 *spec*RExBAD strain provided by Ghigho and coworkers (47). In the resulting fragment, the *erpA* gene is under the control of the pBAD promoter. Replacement of the *wt* allele by the arabinose-inducible *erpA* version was performed as described by Datsenko and Wanner (48), except that arabinose was added in the plate. PCR analysis confirmed that the wild-type *yadQ-erpA* region had been exchanged with the chimeric region described above. P1 was used to move this allele into MG1655, yielding the LL401 strain.

The LL402 strain was constructed as follows. The chloramphenicol resistance gene *cat* was amplified by PCR with primers ΔEs/ΔEas homologous to the end of the *yadQ* and the beginning of the *yadS* coding sequences. Recombinant clones were selected under anaerobiosis in rich medium containing chloramphenicol. Chromosomal DNA was isolated from the mutants obtained, and the structure of the rearranged locus was confirmed by using a series of PCRs with primers complementary to *cat* (CATv) and to the regions adjacent to the site of its insertion (V5/V3). P1 was used to move this allele into MG1655, yielding the LL402 strain.

The LL405 strain was constructed as follows. The MVA-dependent pathway encoding genes were transduced from strain EcAB1–5 (40) into MG1655 by using a Kan^R-linked marker and the resulting strain, MG1655 MVA$^+$, used as a recipient for exchanging wild-type *erpA* with the *yadQ-cat-yadS* fragment as described above. Cam^R was selected under anaerobiosis and subsequently checked for O_2 sensitivity and for actual DNA exchange by PCR using V5/V3 oligonucleotides.

Purification of ErpA. The *E. coli* BL21(DE3) strain was transformed with pET/ErpA vector. Expression was induced for 4 h with 0.4 mM isopropyl β-D-thiogalactoside to exponentially growing cells in LB medium containing 100 μg/ml ampicillin at 37°C. The bacterial pellet (5.5 g per 2 liters) was resuspended in buffer A (0.1 M Tris·HCl, pH 8/0.1 M NaCl) and sonicated before ultracentrifugation at 245,000 × *g* for 90 min at 4°C. The supernatant was treated with DNase I and 10 mM $MgCl_2$ at 4°C for 45 min, and, after centrifugation at 10,174 × *g* for 30 min at 4°C, 340 mg of soluble proteins was loaded onto a 10-ml Ni-NTA affinity column (Qiagen, Valencia, CA) equilibrated with buffer A. The ErpA protein was eluted with buffer A containing 0.2 M imidazole. The ErpA-containing fractions were mixed with ammonium sulfate (60% saturation) for 1 h at 4°C. After centrifugation for 30 min at 10,174 × *g*, the pellet was resuspended in buffer B (50 mM Tris·HCl, pH 8/50 mM NaCl) and desalted onto a Nap-10 column (Amersham Biosciences, Piscataway, NJ). This protocol allowed for the purification of ≈80 mg of ErpA from 340 mg of bacterial extracts. Protein concentration was measured by the Bradford method using bovine serum albumin as a standard. Iron and sulfide were quantitated by the methods of Fish (49) and Beinert (50), respectively.

Iron and Sulfide Binding to ErpA. The following procedures were carried out anaerobically inside a glove box at 18°C [B553 (NMT); Jacomex, Dagneux, France]. ApoErpA was obtained by irradiation of the as-isolated protein with a 10-fold molar excess of decay-accelerating factor in the presence of 20 mM EDTA overnight. Deazaflavin and EDTA were removed by passing the protein through a MicroBioSpin 6 desalting column (Bio-Rad, Hercules, CA). ApoErpA was then incubated in buffer D (buffer A containing 5 mM DTT) for 3–4 h with a 3- to 4-fold molar excess of both Na_2S (Fluka) and $Fe(NH_4)_2(SO_4)_2$ (Aldrich). Then, to remove unspecific bound iron, 2–5 mM EDTA was added to the solution and, after 30 min of incubation, the protein were desalted on a Nap-25 column (Amersham Biosciences) and concentrated on an Amicon Microcon filter (Millipore, Billerica, MA). For Mössbauer analysis, apoErpA (1.1 mM) was mixed with 15 μM IscS and 10 mM L-cysteine (Aldrich) in buffer D, and 3 mM $^{57}FeCl_3$ was then added to the solution. After 4 h incubation, the reconstitution procedure was completed as described above.

Purification of IspG. The *E. coli* BL21(DE3) strain was transformed with pET/IspG vector. The cells were grown to midlog phase in LB medium containing 100 μg/ml ampicillin at 37°C. Expression was then induced by adding 0.5 mM isopropyl β-D-thiogalactoside at 20°C. Cells were harvested after overnight induction and lysed by sonication in binding buffer C (0.1 M Tris·HCl, pH 8/0.25 M NaCl).

The lysate was centrifuged at 245,000 × *g* for 90 min at 4°C, and the supernatant was treated with 3% streptomycin sulfate at 4°C for 45 min. After centrifugation at 10,174 × *g* for 30 min at 4°C), soluble proteins were loaded on a 10-ml Ni-NTA affinity column (Qiagen) equilibrated with buffer C. The IspG-His protein with eluted with buffer C containing 0.5 M imidazole. The IspG-containing fractions were mixed with ammonium sulfate (50% saturation) for 1 h at 4°C. After centrifugation for 30 min at 10,174 × *g*, the pellet was resuspended in buffer B and desalted on a Nap-10 column (Amersham Biosciences) before being concentrated on a Amicon Microcon filter (Millipore).

[Fe–S] Cluster Transfer From ^{57}Fe-Reconstituted ErpA to apoIspG. All of the following procedures were made anaerobically in the glove box at 18°C. IspG, isolated in its apo-form, was incubated for 1 h in buffer E (buffer B containing 5 mM DTT) with a 2.2-fold molar excess of ^{57}Fe-reconstituted ErpA. The proteins were then separated on a Superdex 75 HR 10/30 (Amersham Biosciences) equilibrated with buffer E. The collected fractions were analyzed by SDS/PAGE and UV-visible spectroscopy. The fractions containing pure IspG as judged from SDS/PAGE analysis were concentrated on Microcon before being analyzed by Mössbauer spectroscopy.

Spectroscopy Analysis. UV-visible spectra were recorded with a Uvikon XL spectrophotometer (BioTek Instruments, Winooski, VT). Zero field ^{57}Fe-Mössbauer spectra were recorded by using a 400-μl cuvette with a spectrometer operating in constant acceleration mode using a cryostat (Oxford Instruments, Oxon, U.K.) that allowed temperatures from 1.5 to 300 K and a ^{57}Co source in rhodium. Isomer shifts are reported relative to iron foil at room temperature.

Quinone Extraction and Analysis. Cultures were grown overnight under fermentative conditions, i.e., under anaerobiosis and with glucose. Frozen pellets were resuspended in 2 ml of water and quenched with 6 ml of ice-cold 0.2 M $HClO_4$ in methanol. Six milliliters of petroleum ether (40–60°C) was then added to the mixture and vortex-mixed for 1 min. After the mixture had been centrifuged at 900 × *g* for 1 min, the upper petroleum ether phase was removed, transferred to a test tube, and evaporated to dryness under a flow of nitrogen. Another 6 ml of petroleum ether was added to the lower phase, and the vortex-mixing and centrifugation steps were repeated. The upper phases were combined. After evaporation to dryness, extracts could be stored for at least 7 days under nitrogen at −20°C without any detectable autooxidation. Immediately before use, the extracted ubiquinone/ubiquinol was resuspended with a glass rod in 80 μl of ethanol and analyzed in an HPLC system (LKB gradient pump 2249 system with an LKB 2151 variable wavelength monitor; Amersham Pharmacia) containing a reversed-phase Lichrosorb 10 RP 18 column (Chrompack; Bergen op Zoom, The Netherlands) with a 4.6-mm internal diameter and a length of 250 mm. The column was equilibrated with a 1:1 (vol/vol) ratio of ethanol/methanol, and this mixture was used as the mobile phase. The flow rate was set at 1 ml/min. Detection of the quinones was carried out at 290 nm for ubiquinones, at 248 nm for menaquinones, and at 270 nm to record all quinones simultaneously. The amounts of all quinones were calculated from the peak areas using UQ_{10} and MK_4 as standards according to the method applied by Shestopalov *et al.* (51). Methanol, ethanol, and petroleum ether were of analytical grade. Peaks were identified by UV-visible spectral analysis and mass spectral analysis. A UV-visible spectrum of DMK_8 was obtained from Moscow State University (Moscow, Russia). For mass spectral analysis, fractions collected from the HPLC were evaporated under nitrogen and redissolved into 89% acetonitrile/10% water/1% formic acid (vol/vol) (LC-Grade; Merck, Frankfurt, Germany). The fractions were analyzed by off-line nanoelectrospray mass spectrometry using coated Picotips (Econo12; New Objective, Woburn, MA) on an electrospray ionization quadrople time-of-flight mass spectrometer (Micromass; Waters, Manchester, U.K.). Ions selected for MS/MS collided with argon in the hexapole collision cell. Data processing and evaluation were performed with Masslynx software (Micromass; Waters).

We thank members of F.B.'s group for fruitful discussions, Drs. J. M. Ghigo and C. Beloin (Institut Pasteur, Paris) for a generous gift of strains and plasmids, Drs. M. Ansaldi and A. Magalon for their interest in this study, and Dr. A. V. Bogachev for the DMK_8 spectrum. This work was supported by grants from the Centre National de la Recherche Scientifique, the Centre Energie Atomique, the Université de la Méditerranée (Marseille, France), the Université Joseph Fourier, and the Action Concertée Incitative "Biologie Cellulaire, Moléculaire, et Structurale" from the Ministère de la Recherche. Dr. M. Bekker was supported by a grant from Nederlandse Organisatie voor Wetenschappelijk Onderzoek Aard-en Levenswetenschappen Project 812.05.004.

1. Lill R, Mühlenhoff U (2006) *Annu Rev Cell Dev Biol* 22:457–486.
2. Barras F, Loiseau L, Py B (2005) *Adv Microb Physiol* 50:41–101.
3. Fontecave M, Ollagnier-de Choudens S, Py B, Barras F (2005) *J Biol Inorg Chem* 10:713–721.
4. Johnson DC, Dean DR, Smith AD, Johnson MK (2005) *Annu Rev Biochem* 74:247–281.
5. Beinert H, Holm RH, Munck E (1997) *Science* 277:653–659.
6. Rudolf J, Makrantoni V, Ingledew WJ, Stark MJ, White MF (2006) *Mol Cell* 23:801–808.
7. Huet G, Daffe M, Saves I (2005) *J Bacteriol* 187:6137–6146.
8. Nachin L, El Hassouni M, Loiseau L, Expert D, Barras F (2001) *Mol Microbiol* 39:960–972.
9. Zheng L, White RH, Cash VL, Jack RF, Dean DR (1993) *Proc Natl Acad Sci USA* 90:2754–2758.
10. Kennedy C, Dean D (1992) *Mol Gen Genet* 231:494–498.
11. Mihara H, Kurihara T, Yoshimura T, Esaki N (2000) *J Biochem* 127:559–567.
12. Bonomi F, Iametti S, Ta D, Vickery LE (2005) *J Biol Chem* 280:29513–29518.
13. Agar JN, Krebs C, Frazzon J, Huynh BH, Dean DR, Johnson MK (2000) *Biochemistry* 39:7856–7862.
14. Ollagnier-de Choudens S, Sanakis Y, Fontecave M (2004) *J Biol Inorg Chem* 9:828–838.
15. Ollagnier-de Choudens S, Nachin L, Sanakis Y, Loiseau L, Barras F, Fontecave M (2003) *J Biol Chem* 278:17993–18001.
16. Ollagnier-de Choudens S, Mattioli T, Takahashi Y, Fontecave M (2001) *J Biol Chem* 276:22604–22607.
17. Krebs C, Agar JN, Smith AD, Frazzon J, Dean DR, Huynh BH, Johnson MK (2001) *Biochemistry* 40:14069–14080.
18. Wollenberg M, Bendt C, Bill E, Schwenn JD, Seidler A (2003) *Eur J Biochem* 270:1662–1671.
19. Nachin L, Loiseau L, Expert D, Barras F (2003) *EMBO J* 22:427–437.
20. Outten FW, Wood MJ, Munoz FM, Storz G (2003) *J Biol Chem* 278:45713–45719.
21. Chandramouli K, Johnson MK (2006) *Biochemistry* 45:11087–11095.
22. Silberg JJ, Tapley TL, Hoff KG, Vickery LE (2004) *J Biol Chem* 279:53924–53931.
23. Hoff KG, Silberg JJ, Vickery LE (2000) *Proc Natl Acad Sci USA* 97:7790–7795.
24. Lange H, Kaut A, Kispal G, Lill R (2000) *Proc Natl Acad Sci USA* 97:1050–1055.
25. Takahashi Y, Nakamura M (1999) *J Biochem* 126:917–926.
26. Morimoto K, Yamashita E, Kondou Y, Lee SJ, Arisaka F, Tsukihara T, Nakai M (2006) *J Mol Biol* 360:117–132.
27. Wada K, Hasegawa Y, Gong Z, Minami Y, Fukuyama K, Takahashi Y (2005) *FEBS Lett* 579:6543–6548.
28. Cupp-Vickery JR, Silberg JJ, Ta DT, Vickery LE (2004) *J Mol Biol* 338:127–137.
29. Bilder PW, Ding H, Newcomer ME (2003) *Biochemistry* 43:133–139.
30. Yang J, Bitoun JP, Ding H (2006) *J Biol Chem* 281:27956–27963.
31. Ding H, Harrison K, Lu J (2005) *J Biol Chem* 280:30432–30437.
32. Ding B, Smith ES, Ding H (2005) *Biochem J* 389:797–802.
33. Ding H, Clark RJ (2004) *Biochem J* 379:433–440.
34. Ding H, Clark RJ, Ding B (2004) *J Biol Chem* 279:37499–37504.
35. Djaman OF, Outten W, Imlay JA (2004) *J Biol Chem* 279:44590–44599.
36. Balasubramanian R, Shen G, Bryant DA, Golbeck JH (2006) *J Bacteriol* 188:3182–3191.
37. Johnson DC, Unciuleac MC, Dean DR (2006) *J Bacteriol* 188:7551–7561.
38. Gräwert T, Kaiser J, Zepeck F, Laupitz R, Hecht S, Amslinger S, Schramek N, Schleicher E, Weber S, Haslbeck M, *et al.* (2004) *J Am Chem Soc* 126:12847–12855.
39. Wolff M, Seemann M, Tse Sum Bui B, Frapart Y, Tritsch D, Garcia Estrabot A, Rodriguez-Concepcion M, Boronat A, Marquet A, Rohmer M (2003) *FEBS Lett* 541:115–120.
40. Campos N, Rodriguez-Conception M (2001) *Biochem J* 353:59–67.
41. Seemann M, Wegner P, Schunemann V, Bui BT, Wolff M, Marquet A, Trautwein AX, Rohmer M (2005) *J Biol Inorg Chem* 10:131–137.
42. Ma J, Puustinen A, Wikström M, Gennis RB (1998) *Biochemistry* 37:11806–11811.
43. Björklöf K, Zickermann V, Finel M (2000) *FEBS Lett* 467:105–110.
44. Braun M, Bungert S, Friedrich T (1998) *Biochemistry* 37:1861–1867.
45. Loiseau L, Ollagnier-de Choudens S, Lascoux D, Forest E, Fontecave M, Barras F (2005) *J Biol Chem* 280:26760–26769.
46. Giel JL, Rodionov D, Liu M, Blattner FR, Kiley PJ (2006) *Mol Microbiol* 60:1058–1075.
47. Roux A, Beloin C, Ghigo JM (2005) *J Bacteriol* 187:1001–1013.
48. Datsenko KA, Wanner BL (2000) *Proc Natl Acad Sci USA* 97:6640–6645.
49. Fish WW (1988) *Methods Enzymol* 158:357–364.
50. Beinert H (1983) *Anal Biochem* 131:373–378.
51. Shestopalov AI, Bogachev AV, Murtazina RA, Viryasov MB, Skulachev VP (1997) *FEBS Lett* 404:272–274.

BIOCHEMISTRY